Fate of the Amazon River dissolved organic matter in the tropical Atlantic Ocean

Patricia M. Medeiros[1], Michael Seidel[1,2], Nicholas D. Ward[3,4], Edward J. Carpenter[5], Helga R. Gomes[6], Jutta Niggemann[2], Alex V. Krusche[7], Jeffrey E. Richey[3], Patricia L. Yager[1], and Thorsten Dittmar[2]

[1]Department of Marine Sciences, University of Georgia, Athens, Georgia, USA, [2]Research Group for Marine Geochemistry (ICBM-MPI Bridging Group), University of Oldenburg, Oldenburg, Germany, [3]School of Oceanography, University of Washington, Seattle, Washington, USA, [4]Now at Department of Geological Sciences, University of Florida, Gainesville, Florida, USA, [5]Romberg Tiburon Center, San Francisco State University, Tiburon, California, USA, [6]Lamont-Doherty Earth Observatory, Columbia University, Palisades, New York, USA, [7]Centro de Energia Nuclear na Agricultura, Universidade de São Paulo, Piracicaba, Brazil

Abstract Constraining the fate of dissolved organic matter (DOM) delivered by rivers is a key to understand the global carbon cycle, since DOM mineralization directly influences air-sea CO_2 exchange and multiple biogeochemical processes. The Amazon River exports large amounts of DOM, and yet the fate of this material in the ocean remains unclear. Here we investigate the molecular composition and transformations of DOM in the Amazon River-ocean continuum using ultrahigh resolution mass spectrometry and geochemical and biological tracers. We show that there is a strong gradient in source and composition of DOM along the continuum, and that dilution of riverine DOM in the ocean is the dominant pattern of variability in the system. Alterations in DOM composition are observed in the plume associated with the addition of new organic compounds by phytoplankton and with bacterial and photochemical transformations. The relative importance of each of these drivers varies spatially and is modulated by seasonal variations in river discharge and ocean circulation. We further show that a large fraction (50–76%) of the Amazon River DOM is surprisingly stable in the coastal ocean. This results in a globally significant river plume with a strong terrigenous signature and in substantial export of terrestrially derived organic carbon from the continental margin, where it can be entrained in the large-scale circulation and potentially contribute to the long-term storage of terrigenous production and to the recalcitrant carbon pool found in the deep ocean.

1. Introduction

Rivers can have a significant impact on the biogeochemistry and hydrography of large ocean areas. This is especially true for the Amazon River, by a considerable margin the largest river in the world, accounting for 15–20% of the global freshwater discharge to the ocean [*Meybeck*, 1982; *Richey et al.*, 1986], serving as an important connection between continental hydrology and the tropical Atlantic [*Coles et al.*, 2013]. The Amazon River discharge has a strong seasonal cycle with an average maximum of ~240,000 $m^3 s^{-1}$ in May–June, when low-salinity plume water flows northwestward toward the Caribbean [*Lentz*, 1995]. Lowest average discharge is found in October–November (~80,000 $m^3 s^{-1}$) [*Lentz*, 1995], when a substantial fraction of the Amazon plume water is carried eastward by the North Brazil Current retroflection spreading low-salinity waters into a large area of the tropical Atlantic Ocean [*Fratantoni et al.*, 1995; *Coles et al.*, 2013].

Global riverine discharge represents a substantial source of dissolved organic carbon (DOC) to the oceans [*Hedges et al.*, 1997; *Raymond and Spencer*, 2015], sufficient to support the turnover of DOC throughout the marine environment [*Williams and Druffel*, 1987]. With an average annual export of 22 Tg [*Richey et al.*, 1990] (1 Tg = 10^{12} g) to 27 Tg [*Moreira-Turcq et al.*, 2003] of DOC, the Amazon River is a major source of terrestrially derived organic carbon to the tropical Atlantic Ocean. The Amazon and its tributaries flow for over 6000 km from the Andes (Peru) to the Atlantic, draining an area $> 7 \times 10^6 km^2$ covered by diverse vegetation, including tropical rainforest, inundated floodplain ("várzea") forest, floating grasses, and extensive grassland/savannah [*Hedges et al.*, 1986]. Most rivers in the Amazon system are too turbid for appreciable phytoplankton photosynthesis [*Richey et al.*, 1990; *Hedges et al.*, 1994] to contribute to the otherwise terrestrial character of the riverine dissolved organic matter (DOM). Respiration far exceeds

autochthonous gross primary production in the Amazon River, resulting in a net heterotrophic ecosystem that is fueled primarily by contemporary organic matter originating on land and floodplains [*Mayorga et al.*, 2005; *Abril et al.*, 2014]. A significant portion of the dissolved terrestrial macromolecules seems to be respired within the river by microbes, with the more refractory DOM fraction being discharged into the Atlantic Ocean [*Ward et al.*, 2013]. Although a large fraction of the riverine nutrients exported to the ocean is utilized before the plume leaves the continental margin [*Goes et al.*, 2014], nitrogen-fixing symbionts found in offshore waters provide bioavailable nitrogen that can support considerable phytoplankton blooms [e.g., *Foster et al.*, 2007; *Subramaniam et al.*, 2008; *Yeung et al.*, 2012].

The composition of the DOM directly influences many processes, including its mineralization to inorganic carbon and to nutrients. It also influences bacterioplankton community structure and function [*Crump et al.*, 2009]. Ocean margins have been proposed as major sinks of terrigenous dissolved organic carbon [e.g., *Hedges et al.*, 1997; *Opsahl and Benner*, 1997; *Fichot and Benner*, 2014]. The extent of DOM mineralization in ocean margins directly influences its role in CO_2 exchange with the atmosphere [*Cai*, 2011]. Many previous studies have investigated carbon dynamics in the Amazon River [e.g., *Ertel et al.*, 1986; *Hedges et al.*, 1994; *Amon and Benner*, 1996; *Moreira-Turcq et al.*, 2013; *Ward et al.*, 2013] and in adjacent oceanic waters under the influence of the river plume [e.g., *Sholkovitz et al.*, 1978; *Subramaniam et al.*, 2008]. Because of its immense scale, transformations in the composition of the Amazon River DOM after being delivered to the ocean have important implications for preservation and oxidation of organic matter, and ultimately, for the carbon cycle. Therefore, constraining the western tropical North Atlantic Ocean carbon cycle requires understanding the river and ocean as a continuum rather than as separate entities. Here we use multiple analytical techniques and the first extensive DOM data set collected in the Amazon continuum, extending from the lower reaches of the river to the open ocean, to identify the dominant processes controlling changes in DOM composition in the system and their spatial and temporal variability, as well as to quantify the fraction of terrestrial DOM that the plume delivers to the tropical open ocean.

2. Methods

2.1. Sample Collection

DOM samples were collected in 2010, 2011, and 2012 in the Amazon River to ocean continuum, including the lower reach of the river, from Óbidos (800 km upriver) to the mouth, plume, and open ocean (Figures 1a–1c). Samples were collected during high (May/June 2010, ~300,000 $m^3 s^{-1}$, and July 2012, ~267,000 $m^3 s^{-1}$) and low (September/October 2011, ~110,000 $m^3 s^{-1}$) discharges. Sampling in July 2012 followed a record peak in river discharge (maximum of ~370,000 $m^3 s^{-1}$) and was focused on the plume core between the river mouth and French Guiana (Figure 1c). Riverine sampling included both upstream (Óbidos and Tapajós) and downstream sites (Macapá, Belém), mostly in the central part of the channels, at ~50% of channel depth. In the western tropical North Atlantic Ocean, samples were collected at the surface (~2 m) and below plume (at ~20 m and at ~1000 and 2000 m). At key oceanic stations, more highly resolved vertical profiles were also collected (supporting information Tables S1–S3).

Immediately after collection, riverine (1–2 L) and plume/oceanic (10 L) samples were filtered (0.7 μm Whatman GF/F filters precombusted at 450°C for 5 h and 0.2 μm Pall Supor membranes), and aliquots were collected for DOC analysis. Filtrates were acidified to pH2 (concentrated HCl), and DOM was isolated using solid phase extraction (SPE) cartridges (Agilent Bond Elut PPL) and then eluted with methanol as described in *Dittmar et al.* [2008].

2.2. On Board Incubations

Water incubations were performed on the ship deck in surface seawater flushed plexiglass boxes as in *Medeiros et al.* [2015]. For dark incubations, water samples were first filtered through 0.7 μm combusted GF/F filters, collected into combusted 1 L amber glass bottles in triplicate, wrapped in aluminum foil, and kept submerged for 7 days enclosed by an opaque plastic bag. For photochemical incubation, samples were filtered using 0.7 μm combusted GF/F filters and 0.2 μm membranes and collected in triplicate into 1.5 L quartz flasks with a 500 mL headspace. Flasks were exposed to natural sunlight for 7 days, with the lower part of the flask submerged in a flowing surface seawater bath to regulate temperature. After incubation, all samples were filtered, acidified and DOM was extracted using PPL cartridges as described before.
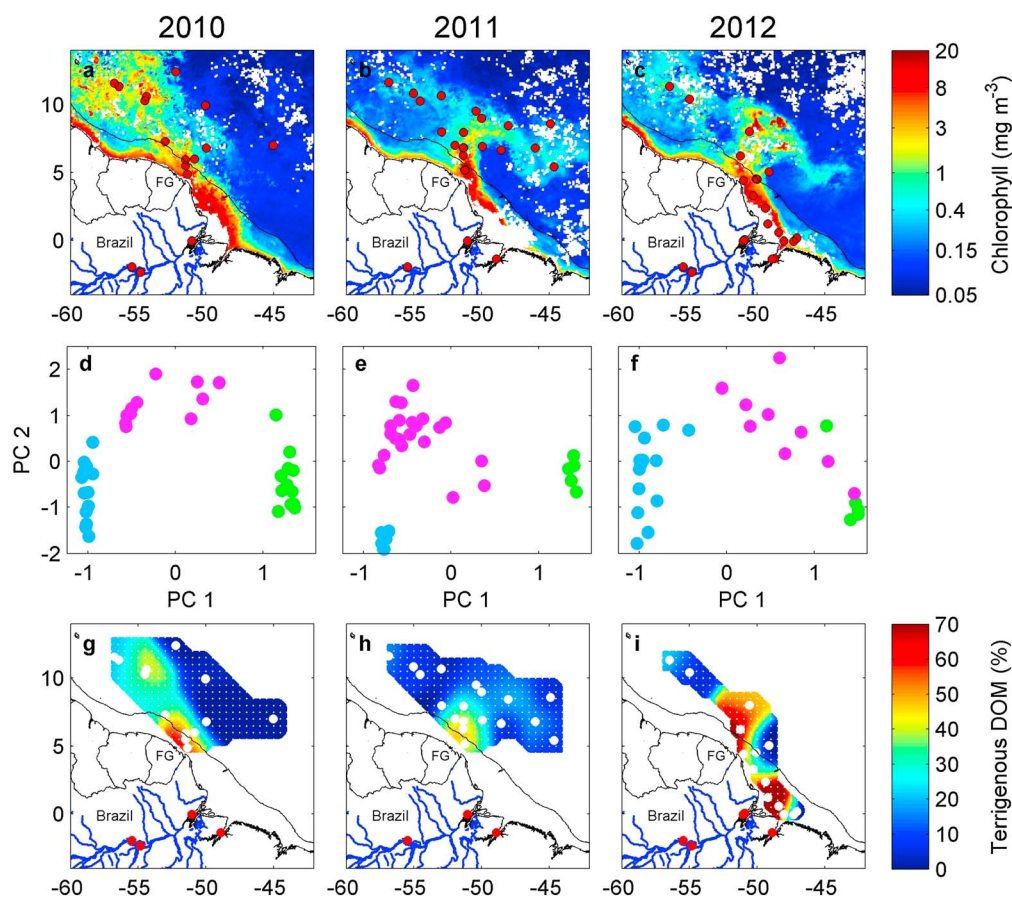
Figure 1. (a–c) Satellite-derived chlorophyll concentration (mg m^{-3}) for May–June 2010, September 2011, and July 2012 from NASA's Aqua-Moderate Resolution Imaging Spectroradiometer with location of stations overlaid. (d–f) Principal component analysis of DOM composition along the Amazon River to ocean continuum based on >4000 molecular formulae. Riverine, plume, and oceanic samples are shown in green, magenta, and blue, respectively. See supporting information Tables S1–S3 for additional information. (g–i) Percentage of DOM that is of terrigenous origin based on two end-member mixing models. End-members of terrigenous and marine sources were extracted from PC 1 of FT-ICR MS-derived DOM composition shown in Figures 1d–1f. Black contour shows the 150 m isobath (shelf break); FG: French Guiana.

2.3. Chemical Analyses

DOC concentrations from water samples and SPE extracts (i.e., evaporated to dryness and redissolved in 10 mL of ultrapure water) were measured with a Shimadzu TOC-V$_{CPH}$ analyzer using potassium hydrogen phthalate as standard for the DOC calibration curve. PPL extraction efficiency across all samples ($n = 101$) was 61 ± 7%. Bulk δ^{13}C ratios of extracted DOC were analyzed with a Finnigan MAT 251 isotope ratio mass spectrometer after pipetting aliquots of the extract onto tin cups and complete drying. All isotopic compositions were expressed relative to the standard Vienna Pee Dee Belemnite. Precision and accuracy were <1‰, and procedural blanks did not yield detectable amounts of carbon isotopes.

The molecular composition of the DOM extracts (in 1:1 water: methanol, yielding a DOC concentration of 15 mg C L^{-1}) was analyzed using a 15 Tesla Fourier transform ion cyclotron resonance mass spectrometer (FT-ICR MS; Bruker Daltonics) with electrospray ionization (negative) as described in detail in *Seidel et al.* [2014]. For each sample, 500 broadband scans were accumulated. All detected compounds had a molecular mass <1000 Da, which is consistent with the observation that most peaks in natural SPE-DOM are detected in the range of 200–800 Da [*Dittmar and Stubbins*, 2014]. Molecular formulae were assigned to peaks with a minimum signal-to-noise ratio of 4. Due to the high degree of similarity between all samples, FT-ICR MS data evaluation was based on normalized peak magnitude.

Principal component (PC) analysis was used to identify the dominant modes of variability in DOM composition in the system. PC analyses were pursued independently for each sampling period. In all cases, PCs 1–3 and results from PC analysis of spatially and temporally uncorrelated random processes were significantly different (95% confidence level) from each other [*Overland and Preisendorfer*, 1982]. PC 4 and higher were not statistically significant in any sampling event. The local fraction of variance explained by each PC at each station was computed as in *Chelton and Davis* [1982]. We emphasize that this study considers the fraction of the DOM that can be extracted by the PPL cartridges and that the fraction of the DOM not retained by the cartridges remained uncharacterized.

Dissolved lignin samples underwent CuO oxidation performed in a CEM Microwave Accelerated Reaction System and were analyzed using a gas chromatograph-time of flight-mass spectrometer (GC-ToF-MS; Agilent 7890A GC, Leco TruToF HT) after derivatization with *N,O*-bis-(trimethylsilyl)trifluoroacetamide (BSTFA) as in *Ward et al.* [2013]. Free lignin monomers were measured by direct injection of the DOM extract onto the GC-ToF-MS after the same BSTFA derivatization. Dissolved black carbon was determined as benzenepolycarboxylic acids after nitric acid oxidation using a UPLC-PDA system (Ultra-performance liquid chromatography - Photodiode array; Waters) as in *Dittmar* [2008]. Particulate organic carbon composition was determined from the 0.7 μm GF/F filters using gas chromatography mass spectrometry as in *Medeiros et al.* [2012].

2.4. Biological Analyses

Phytoplankton cells were concentrated by filtering 2 to 6 L of seawater through 20 μm mesh netting and then backwashing the sample into a 50 mL Falcon tube. Cells were preserved with acidic Lugol's solution. A 1 mL sample (concentrated 15 times when necessary) was then placed in a Sedgwick-Rafter counting chamber. Identification and counting of species was done using a Zeiss Axioskop microscope with a long-working distance objective at 320X magnification. For estimation of chlorophyll *a*, a known volume of the water sample (~5 L) was filtered under low vacuum (<100 mm Hg) through precombusted Whatman GF/F filters. Filters were immediately transferred into glass tubes containing 90% acetone, extracted at −20°C for 24 h, and measured by in vitro fluorometry on a Turner Designs Trilogy Fluorometer using the nonacidification method [*Welschmeyer*, 1994]. The fluorometer was calibrated with pure chlorophyll *a* from Sigma.

For bacterial and community respiration rate measurements, ~3 L of seawater was gravity filtered through a 3 μm membrane filter to separate the free-living bacteria in the water from the particulate matter and larger organisms. Filtrate was gently poured into six sterile pyrex bottles (250 mL) and sealed without headspace. A duplicate set of whole, unfiltered water was also incubated. Samples were kept in the dark at in situ temperatures for 0, 24, or 48 h. Following incubation, duplicates were fixed with 400 μL saturated mercuric chloride solution, resealed, and stored dark and cool until analysis. Samples were analyzed for total dissolved inorganic carbon using a single-operator multimetabolic analyzer connected to a coulometer (precision ~0.5 μmol/kg) [*Johnson et al.*, 1993]. Respiration rates (±95% confidence intervals) were calculated using regression analysis.

2.5. Mass Balance of Terrigenous DOC

A two end-member mixing model

$$\% \text{ terrigenous} = \frac{PC1_{sample} - PC1_{ocean}}{PC1_{river} - PC1_{ocean}} \times 100 \qquad (1)$$

was used to estimate the fraction of the DOM in each sample that was of terrigenous origin. For each sampling event, the end-members of terrigenous ($PC1_{river}$) and marine ($PC1_{ocean}$) sources were extracted from PC1 of FT-ICR MS-derived DOM composition of riverine and oceanic samples (average of green and blue dots in Figures 1d–1f, respectively).

A mass balance approach [*Fichot and Benner*, 2014] was used to estimate the fraction of terrigenous DOC exported from the continental margin in both high (2010) and low (2011) discharge conditions. The amount of terrigenous DOC measured (tDOCm) in the sampled area offshore of the 150 m isobath was calculated as

$$tDOCm = \iint tDOC(x, y) \times V_{ML}(x, y) dx dy \qquad (2)$$

where the terrigenous DOC (tDOC) of any volume of water was calculated as the product of DOC concentration and the fraction of terrigenous material (given by equation (1)). V_{ML} is the volume of water

in the mixed layer, with mixed layer depth determined from potential density profiles collected during the cruises. In order to estimate the amount of terrigenous DOC that would be observed in the same area offshore of the 150 m isobath if no loss occurred (i.e., assuming conservative mixing; tDOCc), we first estimated the total volume of freshwater in the mixed layer using mixed layer depths and the freshwater fraction $f = (S_m - S)/S_m$, where S is the in situ salinity and S_m is the salinity of the marine end-member. tDOCc is then computed as the product between the volume of freshwater in the mixed layer and the bulk DOC concentration at the Amazon River mouth.

Uncertainties in all variables were propagated in the calculations following *Fichot and Benner* [2014]. As in their study, uncertainty associated with the individual measured variables was considered to be ±4% for DOC, ± 20% for mixed layer depth, ±16% for the fraction of terrigenous material (equation (1)), and ±0.02 practical salinity unit (psu) for salinity. To facilitate calculations, all variables were first interpolated into the grid shown in Figures 1g and 1h. Uncertainties associated with each variable after interpolation were assumed to be ±27% for DOC, ± 70% for mixed layer depth, ± 20% for the fraction of terrigenous material, and ±15% for salinity [*Fichot and Benner*, 2014]. Those uncertainties were used to add representative noise levels to all input variables used in the calculation. Additionally, all DOC measurements from near the river mouth (supporting information Tables S1–S2) were used separately in the calculation to incorporate uncertainty in the DOC concentration at the Amazon River mouth. For each measurement available at the mouth, the calculations described above were repeated 10,000 times using the noise-amended inputs. The errors in measured variables and those associated with the interpolation are typically random and are, therefore, largely reduced when propagated in the uncertainty analysis [*Fichot and Benner*, 2014]. The fraction of the terrigenous DOC exported from the Amazon River mouth that is observed offshore of the continental margin for each simulation is then given by the ratio tDOCm/tDOCc × 100.

3. Results and Discussion

The ultrahigh resolution mass spectrometry technique applied here allowed for the assignment of ~4400 molecular formulae in the complex DOM mixture of the Amazon River to ocean continuum in a total of 101 samples (Figures 1a–1c), providing a fingerprint that contains information on its sources and alterations [*Stubbins et al.*, 2010]. Principal component (PC) analysis was used independently for each sampling period (i.e., 2010, 2011, and 2012) to distinguish the dominant patterns of variability in FT-ICR MS-derived DOM composition in the region. In general, samples collected in the river, in the plume, and in the open ocean (either in deep water or far away from the river plume) grouped into distinct clusters (Figures 1d–1f). For all sampling events, riverine samples were characterized on average by depleted $\delta^{13}C$ SPE-DOC signatures (-29.2 ± 0.3‰, -29.6 ± 0.3‰, and -29.7 ± 0.2‰ in 2010, 2011, and 2012, respectively), while oceanic samples presented enriched values (-23.2 ± 0.3‰, -22.0 ± 0.3‰, and -22.8 ± 0.5‰ in 2010, 2011, and 2012, respectively) (supporting information Tables S1–S3). Plume samples had $\delta^{13}C$ SPE-DOC signatures between these two extremes, although samples from low discharge conditions (2011) were characterized by slightly enriched $\delta^{13}C$ ratios (-24.1 ± 1.5‰) compared to high discharge conditions (-25.8 ± 1.4‰ and -27.5 ± 1.0‰ in 2010 and 2012, respectively). Patterns of FT-ICR MS-derived composition of the extracted DOM at the molecular level obtained from the PC analysis for each sampling period were compared with geochemical and biological tracer data ($\delta^{13}C$ SPE-DOC, dissolved lignin, dissolved black carbon, chlorophyll *a*, phytoplankton cell counts, and bacterial respiration) to elucidate the processes controlling variability in DOM composition in the Amazon continuum (Table 1).

3.1. Riverine DOM Dilution and Transport

In 2010 during high river discharge, the first PC (PC1) explained 66% of the total variance in DOM composition and clearly separated riverine and oceanic samples (Figure 1d). This is further illustrated by van Krevelen diagrams, plots in which elemental ratios of O/C (oxygen/carbon) and H/C (hydrogen/carbon) of assigned molecular formulae are displayed. Major chemical classes typically found in DOM have characteristic elemental ratios and, therefore, cluster within specific regions in van Krevelen space [*Kim et al.*, 2003]. For example, highly aromatic compounds show low O/C and low H/C ratios (and therefore cluster on the lower left corner of the diagram), whereas unsaturated aliphatic molecules are generally characterized by medium to high H/C ratios [*Šantl-Temkiv et al.*, 2013; *Seidel et al.*, 2014]. We compared a van Krevelen

Table 1. Interpretation of Principal Components for the Different Sampling Periods[a]

Principal Component	2010	2011	2012
PC1	Dilution (66%)	Dilution (61%)	Dilution (62%)
PC2	Phytoplankton (8%)	Photochemistry (7%)	Phytoplankton (7%)
PC3	Photochemistry (5%)	Phytoplankton (7%)	Biodegradation (6%)

[a]Percentage of total variance explained by each mode is shown in parenthesis.

diagram of the loading of PC1 (Figure 2a, which shows the change in DOM composition in all samples captured by the first mode) with a van Krevelen diagram where only molecular formulae found exclusively in the river end-member (not in the open ocean) and exclusively in the open ocean end-member (not in the river) are plotted (Figure 2b). By plotting only molecular formulae found exclusively in the end-members, the diagram illustrates the differences in DOM composition between river and ocean. The remarkable agreement between the two diagrams supported the interpretation that PC1 separates riverine and oceanic samples according to their distinctive DOM compositions. Compounds found only in the open ocean had significantly higher H/C ratios compared to compounds found only in riverine samples (1.31 ± 0.14 compared to 0.88 ± 0.22). Compounds only present in the river were more aromatic on average (Table 2), agreeing with previous studies that have shown that riverine sources add aromatic compounds to the coastal ocean [e.g., *Mannino and Harvey*, 2004; *Ziolkowski and Druffel*, 2010].
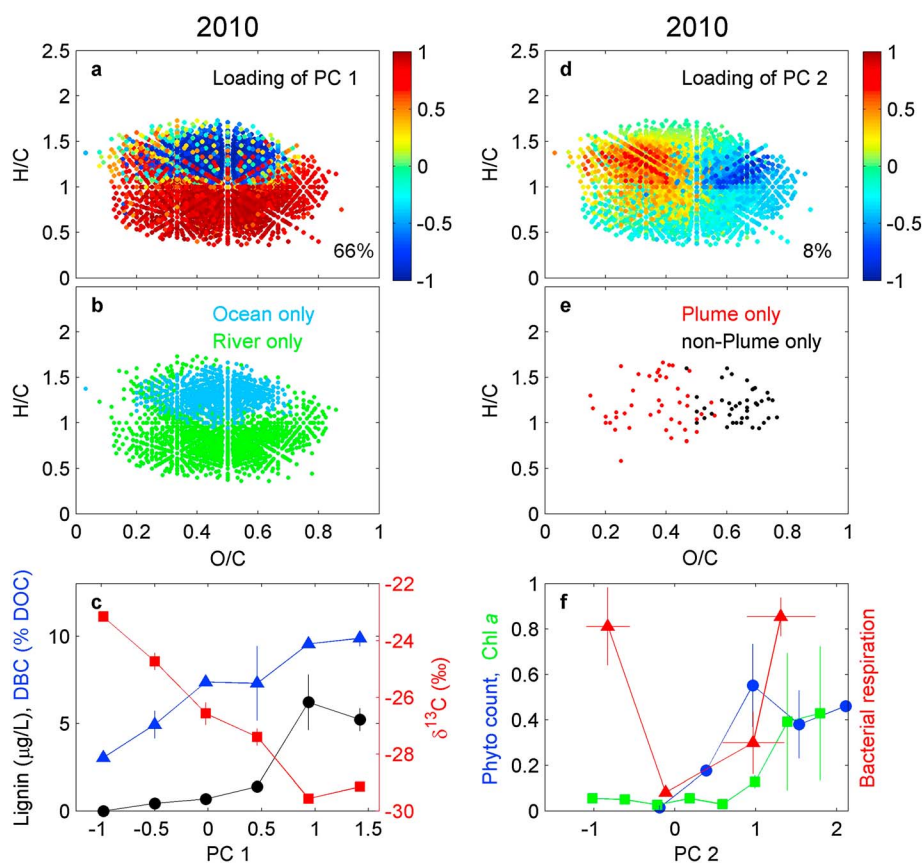

Figure 2. (a) Van Krevelen diagram with loadings of PC 1 during 2010 color coded. (b) Van Krevelen diagram with compounds found exclusively in the ocean or in the river. (c) Relation between PC 1 and dissolved lignin concentrations, dissolved black carbon, and $\delta^{13}C$ of the SPE-DOC. (d) Van Krevelen diagram with loadings of PC 2 during 2010 color coded. (e) Van Krevelen diagram with compounds found exclusively in the plume (plume only) or exclusively in the river and ocean (non-plume only). (f) Relation between PC 2 and phytoplankton cell counts, chlorophyll *a*, and bacterial respiration, normalized to their respective maximum values. Error bars are standard deviations for each bin (in some cases, the error bar is smaller than the size of the symbols).

Table 2. Characteristics of DOM Molecules for Groups Identified by Principal Component Analysis[a]

	End-Members		Processes Modifying DOM Composition[b]		
	Terrestrial	Oceanic	Phytoplankton	Photochemistry	Bacteria
Molecule mass (Da)	422 ± 131	431 ± 91	409 ± 107	297 ± 73	335 ± 102
Carbon	20.7 ± 6.0	19.9 ± 4.1	21.9 ± 4.8	14.8 ± 3.9	17.6 ± 5.6
Hydrogen	18.4 ± 8.0	26.0 ± 5.9	27.3 ± 7.0	22.1 ± 6.6	24.6 ± 8.4
Oxygen	9.5 ± 4.2	9.4 ± 2.9	7.3 ± 3.0	6.0 ± 1.8	6.0 ± 2.5
O/C ratio	0.46 ± 0.15	0.47 ± 0.11	0.32 ± 0.09	0.42 ± 0.13	0.35 ± 0.15
H/C ratio	0.88 ± 0.22	1.31 ± 0.14	1.24 ± 0.11	1.48 ± 0.15	1.40 ± 0.20
Aromaticity index (AI*)	0.51 ± 0.16	0.22 ± 0.13	0.32 ± 0.09	0.16 ± 0.12	0.22 ± 0.15

[a]Given are means $\pm$ standard deviation; AI* = $(1 + C - 0.5O - S - 0.5H)/(C - 0.5O - S - N - P)$ [*Koch and Dittmar*, 2006].
[b]Molecular formulae enriched by each process.

To identify the processes behind such differences in composition, we correlated PC1 with well-known tracers used to distinguish inputs from terrestrial sources to the marine environment. For example, PC1 was highly correlated with δ^{13}C SPE-DOC signatures ($r = -0.97$, $p < 0.05$), concentrations of dissolved lignin phenols ($r = 0.88$, $p < 0.05$; a traditional vascular plant biomarker) [*Ertel et al.*, 1986; *Opsahl and Benner*, 1998], and dissolved black carbon ($r = 0.97$, $p < 0.05$; dissolution products of thermogenic DOM produced on land during biomass burning and subsequently delivered to the sea; *Jaffé et al.* [2013] here encompassing ~10% and ~3% of the DOC in the river and in the ocean, respectively; supporting information Table S1) (Figure 2c). Thus, the PC1 was related to gradients in DOM source along the continuum associated with terrigenous versus oceanic inputs.

Repeating this analysis using observations from low and very high discharge conditions (2011 and 2012, respectively) produced nearly identical results. PC1 explained 61% and 62% of the total variance in DOM composition in 2011 and 2012, respectively (supporting information Figure S1), and again separated riverine and oceanic samples (Figures 1e and 1f). In both years, PC1 was highly correlated with δ^{13}C SPE-DOC signatures and with the fraction of molecular formulae presenting aromaticity index ≥ 0.67 (supporting information Figures S1c and S1f), an indicator of condensed aromatic structures [*Koch and Dittmar*, 2006], showing once again that, in all sampling events, PC1 captured changes in DOM composition along the continuum from riverine and marine organic matter contributions.

Since PC1 explained 61–66% of the total variance in DOM composition along the Amazon continuum in all sampling periods, regardless of river discharge, end-member mixing dominated, and DOM composition was therefore primarily dictated by the dilution of Amazon River waters into the ocean. A large fraction of the Amazon River DOM was transported to the north with little alteration during both low and high discharge conditions. This finding is consistent with observations that much of the labile DOM is consumed within the river, leading to the export of the more refractory fraction [*Raymond and Bauer*, 2001; *Ward et al.*, 2013]. However, a two end-member mixing model (equation (1)) revealed that the fraction of the DOM in the plume that was of terrigenous origin varied with discharge. Plume DOM had a signature that was ~50% terrestrial off French Guiana (~500 km to the northwest of the river mouth) in 2010 at high discharge (Figure 1g). That increased to over 60% in 2012 during very high discharge conditions (Figure 1i). In 2011, during low discharge conditions, plume DOM had a signature that was ~40% terrigenous off French Guiana (Figure 1h), indicating a smaller contribution from terrestrially derived DOM. Computing the fraction of terrigenous material using δ^{13}C SPE-DOC signatures, instead of PC1 values, yielded results similar to those shown in Figures 1g–1i (supporting information Table S4). This is expected since PC1 values and δ^{13}C SPE-DOC ratios were highly correlated (Figure 2c and supporting information Figure S1).

These results indicated the presence of a significant amount of terrigenous DOM off the coast of French Guiana, which was then transported northwestward during spring (Figure 1g) or eastward by the North Brazil Current retroflection [*Fratantoni et al.*, 1995] during fall (Figure 1h, see also Figure 1b). A comparison of results from 2010 and 2011, when approximately the same spatial area was sampled, revealed that the region in the tropical Atlantic Ocean with a terrestrial DOM signature $> 20\%$ was much larger during high discharge (~410,000 km^2) than during low river flow (~110,000 km^2). The mass balance approach
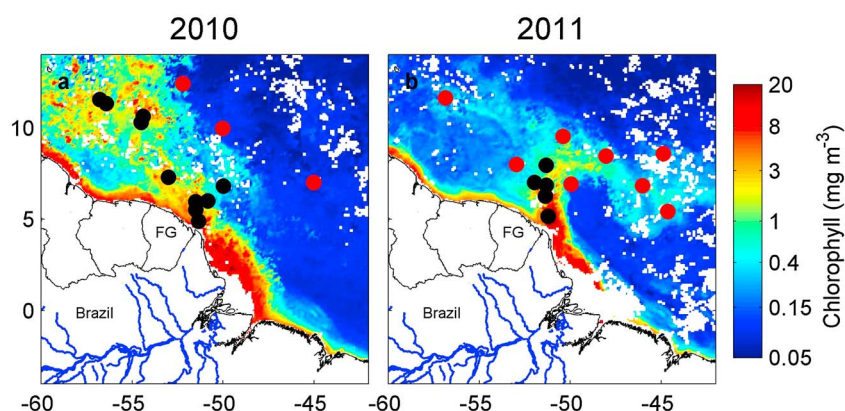
Figure 3. Satellite-derived chlorophyll concentration (mg m^{-3}) for (a) May–June 2010 and (b) September 2011. Black (red) circles indicate stations in which the PC associated with phytoplankton blooms explains a statistically significant larger (smaller) fraction of the local variance compared to the PC associated with DOM changes due to photochemical transformations. FG: French Guiana.

[*Fichot and Benner*, 2014] revealed that the fraction of terrigenous DOC exported from the continental margin was $76 \pm 15\%$ during high river flow in 2010, and $50 \pm 10\%$ during low river flow in 2011. This showed that large amounts of terrigenous and refractory DOM from the Amazon River are exported from the continental margin, extending to a vast area of the western tropical Atlantic Ocean.

3.2. Processes Changing DOM Composition

Despite the stable character of a large component of the Amazon DOM delivered to the continental margin, a significant fraction (~35–40%) of the variance in DOM composition along the continuum was explained by processes other than dilution. In 2010 during high discharge conditions, the second PC (PC2) separated plume samples from riverine and oceanic samples (Figure 1d), revealing a pattern of DOM composition in the plume that is different from that in the river and the open ocean. Analyses of molecular formulae found exclusively in plume samples versus exclusively in nonplume (i.e., riverine and oceanic) samples (Figure 2e) showed a pattern consistent with the loadings of PC2 (Figure 2d; compare location in van Krevelen space—i.e., O/C versus H/C ratios—of large positive values of loadings of PC2 to compounds found exclusively in the plume, and large negative values of loadings of PC2 to compounds found exclusively in nonplume samples). Therefore, PC2, which accounts for 8% of the total variability in DOM composition along the river continuum at high discharge (2010), may be related to alteration processes, capturing the autochthonous generation of molecules in the plume.

In order to elucidate processes that could have driven changes in DOM composition within the high discharge plume, we used in situ microbial data. While PC2 was not significantly correlated (at the 95% confidence level) with bacterial respiration along the continuum ($r = -0.02$; Figure 2f), phytoplankton cell counts and chlorophyll *a* concentrations (a proxy for phytoplankton biomass) were significantly correlated with PC2 ($r = 0.79$ and 0.83, $p < 0.05$; Figure 2f), suggesting that PC2 was related to changes in DOM composition associated with algal blooms. Indeed, computing the local fraction of the variance explained by each PC (as in *Chelton and Davis* [1982]) in 2010 revealed that PC2 is most important along the core of the plume, in locations where chlorophyll concentrations were relatively high (black circles in Figure 3a). This interpretation was further supported by recent experiments in which the DOM composition of exudates from phytoplankton cultures grown in laboratory was analyzed by FT-ICR MS [*Landa et al.*, 2014]. The experiments revealed that the phytoplankton-derived DOM (exudates) was characterized by compounds with O/C < 0.5 and H/C > 1, approximately the same location in van Krevelen space where large positive values of the loadings of PC2 were seen (Figure 2d and Table 2). In addition, analysis of the composition of the particulate organic carbon showed saccharides and low molecular weight fatty acids, i.e., short-lived biomarker indicators of algal inputs [*Ahlgren et al.*, 1992; *Medeiros et al.*, 2012], as the major compounds present in those samples (supporting information Figure S2). Together, these results suggested that the extensive phytoplankton blooms observed in the plume (e.g., Figure 1a) are most likely responsible for adding compounds to the DOM pool, thereby modifying the DOM composition in the Amazon plume.
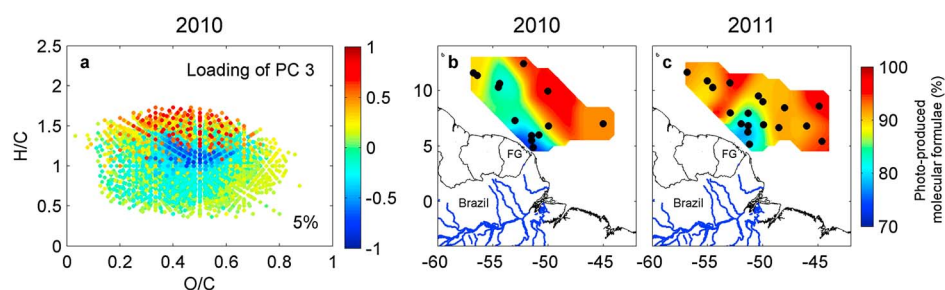
Figure 4. (a) Van Krevelen diagram with loadings of PC 3 during 2010 color coded. (b, c) Percent of molecular formulae observed in each sample that were also produced during an experiment in which water from the river mouth was exposed to natural sunlight. FG: French Guiana.

A similar pattern of variability was observed in 2011 (PC3) and 2012 (PC2) during low and very high discharge conditions, respectively (supporting information Figure S3), explaining ~7% of the total variance in DOM composition variability in each case. Similar to the 2010 data, the PC interpreted to be associated with phytoplankton blooms during low discharge conditions (2011; PC3 in supporting information Figure S3a) was most important in areas of enhanced chlorophyll concentrations in satellite images (Figure 3b).

Away from the core of the plume in open waters (red circles in Figures 3a and 3b), where chlorophyll concentrations were low, a relatively large fraction of the local variance was explained by a different PC. Van Krevelen diagrams of the loadings of that PC (i.e., PC3 in 2010 and PC2 in 2011) were similar to each other during high and low river discharge (Figure 4a and supporting information Figure S4), explaining 5–7% of the total variance in DOM composition variability. The pattern captured by the loadings of the PC (increased relative abundance of compounds with high H/C ratios) was different from the pattern described before associated with phytoplankton inputs, indicating that the variability must be related to some other biogeochemical processes. Since that pattern of variability was observed in clearer waters away from the plume core (Figures 3a and 3b), one possible driver is photochemical reactions. Indeed, photochemical reactions of DOM often lead to the enrichment of compounds with high H/C ratios [*Stubbins et al.*, 2010; *Chen et al.*, 2014; *Medeiros et al.*, 2015].

To test this hypothesis, molecular formulae present in surface samples collected at high (2010) and low (2011) river flow were compared to molecular formulae of compounds produced during an experiment in which Amazon River mouth water ($S \sim 0$) was exposed to natural sunlight for about 7 days. Away from the plume core where the PC was most significant (Figures 3a and 3b), nearly all molecular formulae produced during the irradiation experiment were also observed in samples at both high and low discharges (Figures 4b and 4c). At the core of the plume near French Guiana, where the PC was relatively less important (Figures 3a and 3b), only ~70% of the molecular formulae photochemically produced in the irradiation experiment were observed (Figures 4b and 4c). This finding was consistent with the hypothesis that photochemical transformations captured by PC3 in 2010 and PC2 in 2011 (Figure 4a and supporting information Figure S4, respectively) make a significant contribution to changes in DOM composition in surface samples less influenced by Amazon River waters, presumably because of increased water clarity and light penetration.

These results suggested that both phytoplankton-derived DOM inputs and photochemical reactions play important roles in contributing to the DOM composition associated with the Amazon plume. The contribution of each process varied seasonally, however, influenced by both river discharge and mean circulation patterns. As such, the area where phytoplankton inputs were more important extended toward the Caribbean during spring along the core of the plume trajectory. During fall, the major contribution occurred in the retroflection region (Figures 3a and 3b). In both cases, this was consistent with the general water circulation pattern in the region [*Lentz*, 1995; *Fratantoni et al.*, 1995]. The process consistent with photochemical transformation, on the other hand, was more significant at stations located on the border of or away from the seasonally varying plume trajectory (Figures 3a and 3b), where clearer waters and low phytoplankton abundance presumably increased its relative importance. We note that this mode of variability was only observed in 2010 and 2011. This is most likely because sampling in 2012 was concentrated in the core of the plume (Figure 1c), with very few samples collected in clear offshore waters.
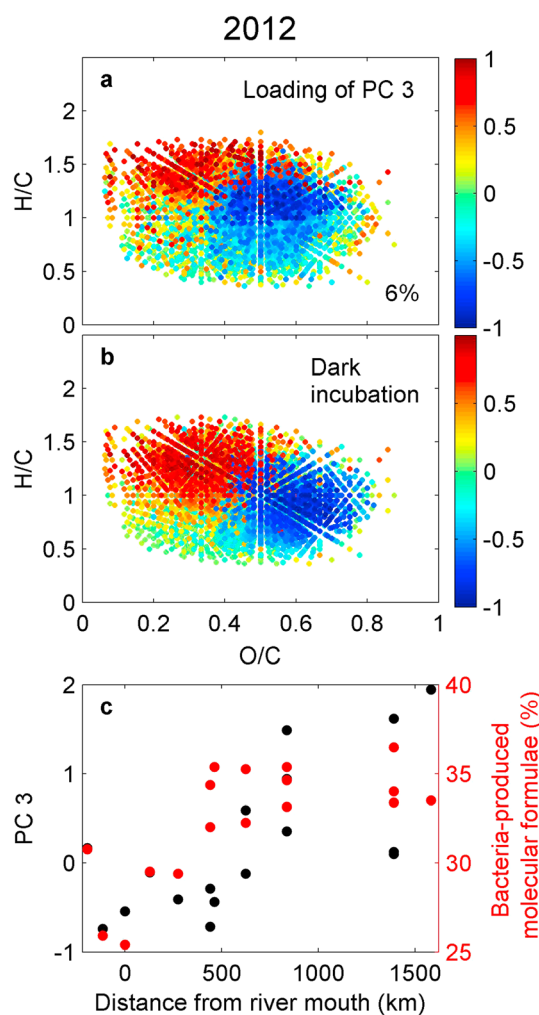
Figure 5. (a) Van Krevelen diagram with loadings of PC 3 during 2012 color coded. (b) Van Krevelen diagram showing compounds that were consumed (blue) and produced (red) during an experiment in which water from the river mouth was incubated in the dark. (c) PC 3 as a function of distance from the river mouth (black circles, see Figure 1c for location). Also shown (red circles) are percent of molecular formulae that had been produced during dark incubation that were observed in each sample.

Even though observations in 2012 extended all the way to the mouth of the Amazon River (Figure 1c), the dominant patterns of variability extracted by the PC analysis (supporting information Figures S1 and S3) were similar to the other years. This suggested that although the 2010 and 2011 cruises did not extend to the river mouth, sampling was sufficient to capture the dominant patterns of DOM composition variability in the system.

Extending the sample collection toward the river mouth in 2012 allowed us to identify an additional pattern of variability in DOM composition, however. The van Krevelen diagram of the loadings of PC3 (6% of the total variability in DOM composition in the continuum) obtained using observations from 2012 (Figure 5a) showed a pattern that is different from those observed in the previous years (when sampling was not extended to the river mouth). To identify the process driving this pattern of variability, the van Krevelen diagram was compared with results from bacterial dark incubation experiments conducted using water collected at the river mouth in 2012. The experiment revealed a pattern that is notably similar to that depicted in PC3 in 2012. The preincubation DOM was relatively enriched with compounds with high O/C and low H/C ratios, while the postincubated DOM was enriched with compounds with low O/C and high H/C ratios (Figure 5b), which is consistent with previous studies that have shown that biodegradation selectively removes compounds with higher O/C ratios [*Kim et al.*, 2006]. PC3 increased as a function of distance from the river mouth (Figure 5c; $r = 0.68$, $p < 0.05$) revealing that the component captured a similar shift in the DOM composition, from compounds with high O/C and low H/C ratios near the river mouth to compounds with low O/C and high H/C at 1000–1500 km from the river mouth. Additionally, the fraction of the molecular formulae enriched in the dark incubation experiments as a result of bacterial degradation that was observed in the samples increased with distance from the river mouth (Figure 5c; $r = 0.69$, $p < 0.05$). This suggested that the changes in DOM composition as the water was transported northward from the river mouth toward the Caribbean captured by PC3 in 2012 were related to bacterial degradation. It is important to point out that similar microbial-derived changes in DOM composition may have occurred in 2010 and 2011. The lack of observations near the river mouth in those years would not allow for such pattern of variability to be extracted by the PC analysis, however.

3.3. Implications for DOM Alterations and Export

Collectively, the characterization of the DOM composition along the Amazon continuum revealed that a large fraction of the Amazon River DOM was stable in the coastal ocean, even on a very detailed molecular formula level. Dilution of riverine waters into the ocean explained most of the variability in DOM composition in the system at both high and low discharges, with the plume DOM having a strong terrigenous signature over a

vast area of the western tropical Atlantic Ocean. This is surprising, considering that previous studies have shown that terrestrial DOM is removed rapidly and efficiently in ocean margins [*Hedges et al.*, 1997; *Opsahl and Benner*, 1997; *Hernes and Benner*, 2003], suggesting that coastal zones act as major sinks of terrigenous DOC between land and ocean [*Fichot and Benner*, 2014].

In the Mississippi River plume, quantitative estimates showed that less than 50% of the terrigenous DOC resists biomineralization and/or photomineralization to CO_2 inshore of the 200 m isobath along the coastal margin [*Fichot and Benner*, 2014]. Since it is possible that the terrigenous material will continue to be degraded as it is transported offshore, the fraction of the terrigenous material from the Mississippi River that is exported from the continental margin is likely to be even smaller. In the Amazon River to ocean continuum, about 76% of the terrigenous DOM delivered to the ocean by the river during high discharge conditions was exported from the continental margin. The fraction of terrigenous material exported during low discharge conditions was relatively smaller at ~50%, indicating a large seasonal variability in the export. With only two sampling events, we cannot compute the average fraction of the terrigenous DOM exported from the continental margin on an annual basis. We note, however, that the DOC concentrations in water samples from the Amazon River vary over the year largely following the variability in river discharge. Bulk DOC concentrations are highest at the beginning of high discharge and lowest during low discharge conditions [*Ward et al.*, 2013], suggesting that the DOC flux from the Amazon River to the ocean is larger during the high discharge season. If this is true, it implies that the fraction of the terrigenous material exported from the continental margin averaged on an annual basis using the DOC flux as weights is likely to be closer to the fraction computed during high discharge conditions (76 ± 15%) than to the value computed during low discharge conditions (50 ± 10%).

These results suggest that a large fraction of the DOM discharged by the Amazon River to the Atlantic Ocean seems to be quite stable over the continental margin, possibly because it has already been thoroughly biologically degraded in the soils and fluvial waters of the Amazon prior to export [*Ward et al.*, 2013]. Perhaps more importantly, plume waters are exported from the continental margin relatively quickly. Recent numerical model simulations and analysis of drifter trajectories revealed that the mean age of drifters within the plume is 2–2.5 months [*Coles et al.*, 2013], and drifters released near the river mouth generally leave the continental margin on even shorter time scales (i.e., <30–60 days) [*Limeburner et al.*, 1995; *Coles et al.*, 2013], as they are entrained in the swift and energetic North Brazil Current [*Coles et al.*, 2013]. For comparison, export from the continental margin in the Mississippi River plume occurs on time scales of several months longer [*Fichot and Benner*, 2014]. Therefore, the relatively large fraction of terrigenous material exported from the continental margin in the Amazon plume reported here may be, alternatively, a result of the short residence time of plume waters over the shelf, which would not allow enough time for substantial organic matter degradation to occur. Additionally, the high turbidity (suspended sediment concentrations $> 10\,mg\,L^{-1}$) area of the Amazon River plume generally extends for several hundred kilometers from the river mouth [*Smith and DeMaster*, 1996], which can potentially decrease light penetration and photomineralization of terrigenous organic matter over the coastal region compared to other riverine systems. Since the most recent estimates indicate that the Amazon River exports ~27 Tg of DOC to the ocean each year [*Moreira-Turcq et al.*, 2003], our mass balance calculations suggest that 13–21 Tg yr^{-1} of terrigenous DOC are exported from the continental margin.

It is important to emphasize some of the limitations of the mass balance approach used here. The analysis considered uncertainties in DOC concentration, salinity, mixed layer depth, percentage of terrigenous material, and time variability in DOC concentration at the river mouth. The spatial resolution of the observations offshore of the continental margin is relatively low, however, especially considering the vast extension of the plume and its heterogeneity. This can potentially introduce a bias in the calculation, for example, if a pocket of plume water containing an unusually high or low fraction of terrigenous DOC was sampled. Since we cannot identify if that occurred based on our observations alone, that uncertainty cannot be fully taken into account in the analysis pursued here. Fully incorporating this into the mass balance calculations is dependent on the availability of high resolution, quasi-synoptic observations spanning the vast expansion of the Amazon River plume covering different discharge regimes. Considering the logistic difficulty and expense to obtain such in situ observations, better constraining the fraction of the terrigenous DOC introduced into the ocean by the Amazon River that is exported from the continental margin will possibly depend on the availability of well-calibrated satellite
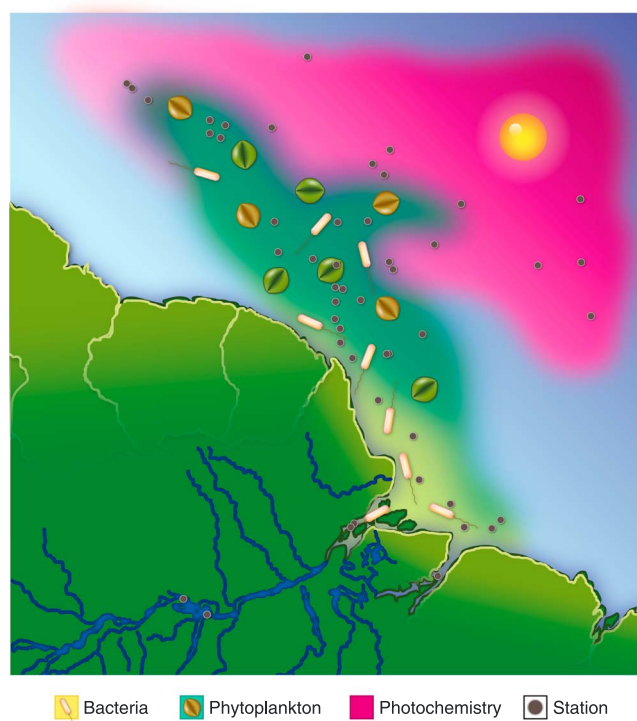
Bacteria Phytoplankton Photochemistry Station

Figure 6. Predominant processes changing DOM composition in the Amazon River to ocean continuum. Bacterial and photochemical transformations and addition of compounds due to phytoplankton blooms act together to change the DOM composition in the Amazon River plume. Although all processes likely occur simultaneously over the entire continuum, spatial variability in their relative importance is observed. Near the river mouth, terrestrial macromolecules are continuously broken down by bacteria (yellow). Far from the river mouth toward the Caribbean during spring or in the retroflection region during fall, large phytoplankton blooms contribute substantially to changing the organic matter composition in the plume by adding new compounds to the DOM (green). In clear waters offshore, away from the low-salinity region under the influence of the Amazon River, the dominant pattern of variability in DOM composition is consistent with transformations due to photochemical reactions (magenta).

algorithms and/or biogeochemical models. Another limitation of the approach used here is that the calculations were based on chemical composition of PPL extracts. Although the extraction efficiency was relatively high at $61 \pm 7\%$ of the DOC, a fraction of the DOM remained uncharacterized.

Once exported from the continental margin, the fate of the terrigenous material remains unconstrained. It is likely that at least some of this material will continue to be modified in the open ocean. Indeed, despite its high stability, we identified three main processes modifying the DOM composition in Amazon plume waters (Table 1), each accounting for 6–8% of the total variability in DOM composition in the continuum. Phytoplankton blooms played an important role in changing the DOM composition by adding new compounds to the DOM pool, especially along the core of the plume. Also important to the compositional changes of DOM as water is transported from the river mouth toward the Caribbean were bacterial transformations. Farther from the river mouth, changes in DOM composition in clear and oligotrophic offshore waters that are consistent with photochemical transformations became more significant. Therefore, DOM composition changes due to inputs from phytoplankton blooms and from bacterial and photochemical transformations

contributed to the makeup of different biogeochemical provinces in Amazon plume waters (Figure 6), imprinting a distinctive change in DOM composition in the Atlantic Ocean. Processes transforming DOM composition have been described in other large river plumes [e.g., *Cadée*, 1984; *Benner and Opsahl*, 2001; *Spencer et al.*, 2009]. Here we identified the molecular signature and the chemical characteristics of the contribution of each of these processes (Table 1) to changes in DOM composition in the Amazon plume under varying river discharges and showed that, although these processes are likely to occur simultaneously along the entire continuum, strong spatial variability in their relative importance is observed (Figure 6). Our analyses also revealed that discharge and mean circulation patterns change both the location and the extent of the dominant biogeochemical provinces.

Lastly, we captured the increase in the fraction of DOM that is of terrigenous origin in the tropical Atlantic Ocean during high river discharge, which was further increased during a record flooding season. Since the Amazon River discharge is predicted to increase in future climate scenarios [*Manabe et al.*, 2004; *Nohara et al.*, 2006], the delivery of terrestrial DOM to the ocean and the export from the ocean margin is likely to be enhanced. The observed input of refractory DOM to ocean waters adjacent to the North Brazil Current, which is known to contribute to meridional oceanic transport [*Fratantoni et al.*, 1995], suggests that a fraction of the Amazon DOM may be entrained into the global overturning circulation [*Kuhlbrodt et al.*, 2007]. In this context, this

study suggests that the Amazon River (and possibly other rivers worldwide) may contribute to the long-term carbon storage of terrigenous production and to the molecularly identified pool of thermogenic and refractory DOM observed throughout the deep ocean [*Dittmar and Paeng*, 2009].

References

Abril, G., et al. (2014), Amazon River carbon dioxide outgassing fuelled by wetlands, *Nature*, *505*, 395–398.

Ahlgren, G., I. B. Gustafsson, and M. Boberg (1992), Fatty acid content and chemical composition of freshwater microalgae, *J. Phycol.*, *28*, 37–50.

Amon, R. M. W., and R. Benner (1996), Photochemical and microbial consumption of dissolved organic carbon and dissolved oxygen in the Amazon River system, *Geochim. Cosmochim. Acta*, *60*, 1783–1792.

Benner, R., and S. Opsahl (2001), Molecular indicators of the sources and transformations of dissolved organic matter in the Mississippi River plume, *Org. Geochem.*, *32*, 597–611.

Cadée, G. C. (1984), Particulate and dissolved organic carbon and chlorophyll a in the Zaire River, estuary and plume, *Neth. J. Sea Res.*, *17*, 426–440.

Cai, W. J. (2011), Estuarine and coastal ocean carbon paradox: CO_2 sinks or sites of terrestrial carbon incineration?, *Annu. Rev. Mar. Sci.*, *3*, 123–145, doi:10.1146/annurev-marine-120709-142723.

Chelton, D. B., and R. Davis (1982), Monthly mean sea-level variability along the west coast of North America, *J. Phys. Oceanogr.*, *12*, 757–784.

Chen, H., A. Stubbins, E. M. Perdue, N. W. Green, J. R. Helms, K. Mopper, and P. G. Hatcher (2014), Ultrahigh resolution mass spectrometric differentiation of dissolved organic matter isolated by coupled reverse osmosis-electrodialysis from various major oceanic water masses, *Mar. Chem.*, *164*, 48–59.

Coles, V. J., M. T. Brooks, J. Hopkins, M. R. Stukel, P. L. Yager, and R. R. Hood (2013), The pathways and properties of the Amazon River plume in the tropical North Atlantic Ocean, *J. Geophys. Res. Oceans*, *118*, 6894–6913.

Crump, B. C., B. J. Peterson, P. A. Raymond, R. M. W. Amon, A. Rinehart, J. W. McClelland, and R. M. Holmes (2009), Circumpolar synchrony in big river bacterioplankton, *Proc. Natl. Acad. Sci. U.S.A.*, *106*, 21,208–21,212.

Dittmar, T. (2008), The molecular level determination of black carbon in marine dissolved organic matter, *Org. Geochem.*, *39*, 396–407.

Dittmar, T., and J. Paeng (2009), A heat-induced molecular signature in marine dissolved organic matter, *Nat. Geosci.*, *2*, 175–179.

Dittmar, T., and A. Stubbins (2014), Dissolved organic matter in aquatic systems, in *Treatise on Geochemistry*, 2nd ed., vol. 12, edited by H. Holland, and K. Turekian, pp. 125–156, Elsevier Science.

Dittmar, T., B. Koch, N. Hertkorn, and G. Kattner (2008), A simple and efficient method for the solid-phase extraction of dissolved organic matter (SPE-DOM) from seawater, *Limnol. Oceanogr. Methods*, *6*, 230–235.

Ertel, J. R., J. I. Hedges, A. H. Devol, J. E. Richey, and M. N. G. Ribeiro (1986), Dissolved humic substances of the Amazon River system, *Limnol. Oceanogr.*, *31*, 739–754.

Fichot, C. G., and R. Benner (2014), The fate of terrigenous dissolved organic carbon in a river-influenced ocean margin, *Global Biogeochem. Cycles*, *28*, 300–318, doi:10.1002/2013GB004670.

Foster, R. A., A. Subramaniam, C. Mahaffey, E. J. Carpenter, D. G. Capone, and J. Zehr (2007), Influence of the Amazon River plume on distributions of free-living and symbiotic cyanobacteria in the western tropical North Atlantic Ocean, *Limnol. Oceanogr.*, *52*, 517–532.

Fratantoni, D. M., E. W. Johns, and T. L. Townsend (1995), Rings of the North Brazil Current: Their structure and behavior inferred from observations and a numerical simulation, *J. Geophys. Res.*, *100*, 10,633–10,654, doi:10.1029/95JC00925.

Goes, J. I., et al. (2014), Influence of the Amazon River discharge on the biogeography of phytoplankton communities in the western tropical north Atlantic, *Progr. Oceanogr.*, *120*, 29–40.

Hedges, J. I., W. A. Clark, P. D. Quay, J. E. Richey, A. H. Devol, and U. d. M. Santos (1986), Compositions and fluxes of particulate organic material in the Amazon River, *Limnol. Oceanogr.*, *31*, 717–738.

Hedges, J. I., G. L. Cowie, J. E. Richey, P. D. Quay, R. Benner, M. Strom, and B. R. Forsberg (1994), Origins and processing of organic matter in the Amazon River as indicated by carbohydrates and amino acids, *Limnol. Oceanogr.*, *39*, 743–761.

Hedges, J. I., R. G. Keil, and R. Benner (1997), What happens to terrestrial organic matter in the ocean?, *Org. Geochem.*, *27*, 195–212, doi:10.1016/S0146-6380(97)00066-1.

Hernes, P. J., and R. Benner (2003), Photochemical and microbial degradation of dissolved lignin phenols: Implications for the fate of terrigenous dissolved organic matter in marine environments, *J. Geophys. Res.*, *108*(C9), 3291, doi:10.1029/2002JC001421.

Jaffé, R., Y. Ding, J. Niggemann, A. V. Vähätalo, A. Stubbins, R. G. M. Spencer, J. Campbell, and T. Dittmar (2013), Global charcoal mobilization from soils via dissolution and riverine transport to the oceans, *Science*, *340*, 345–347.

Johnson, K. M., M. D. Willis, D. B. Butler, W. K. Johnson, and C. S. Wong (1993), Coulometric total carbon dioxide analysis for marine studies: Maximizing the performance of an automated gas extraction system and coulometric detector, *Mar. Chem.*, *44*, 167–187.

Kim, S., R. W. Kramer, and P. G. Hatcher (2003), Graphical method for analysis of ultrahigh resolution broadband mass spectra of natural organic matter, the van Krevelen diagram, *Anal. Chem.*, *75*, 5336–5344.

Kim, S., L. A. Kaplan, and P. G. Hatcher (2006), Biodegradable dissolved organic matter in a temperate and a tropical stream determined from ultra-high resolution mass spectrometry, *Limnol. Oceanogr.*, *51*, 1054–1063.

Koch, B. P., and T. Dittmar (2006), From mass to structure: An aromaticity index for high-resolution mass data of natural organic matter, *Rapid Commun. Mass Spectrom.*, *20*, 926–932, doi:10.1002/rcm.2386.

Kuhlbrodt, T., A. Griesel, M. Montoya, A. Levermann, M. Hofmann, and S. Rahmstorf (2007), On the driving processes of the Atlantic meridional overturning circulation, *Rev. Geophys.*, *45*, RG2001, doi:10.1029/2004RG000166.

Landa, M., et al. (2014), Phylogenetic and structural response of heterotrophic bacteria to dissolved organic matter of different chemical composition in a continuous culture study, *Environ. Microbiol.*, *16*, 1668–1681.

Lentz, S. J. (1995), Seasonal variations in the horizontal structure of the Amazon plume inferred from historical hydrographic data, *J. Geophys. Res.*, *100*(C2), 2391–2400, doi:10.1029/94JC01847.

Limeburner, R., R. C. Beardsley, I. D. Soares, S. J. Lentz, and J. Candela (1995), Lagrangian flow observations of the Amazon River discharge into the North Atlantic, *J. Geophys. Res.*, *100*, 2401–2415, doi:10.1029/94JC03223.

Manabe, S., P. C. D. Milly, and R. T. Wetherald (2004), Simulated long-term change in river discharge and soil moisture due to global warming, *Hydrol. Sci. J.*, *49*, 625–642.

Mannino, A., and H. Harvey (2004), Black carbon in estuarine and coastal ocean dissolved organic matter, *Limnol. Oceanogr.*, *49*, 735–740.

Mayorga, E., A. K. Aufdenkampe, C. A. Masiello, A. V. Krusche, J. I. Hedges, P. D. Quay, J. E. Richey, and T. A. Brown (2005), Young organic matter as source of carbon dioxide outgassing from the Amazonian rivers, *Nature*, *436*, 538–541.

Medeiros, P. M., E. L. Sikes, B. Thomas, and K. H. Freeman (2012), Flow discharge influences on input and transport of particulate and sedimentary organic carbon along a small temperate river, *Geochim. Cosmochim. Acta*, *77*, 317–334.

Medeiros, P. M., M. Seidel, L. C. Powers, T. Dittmar, D. A. Hansell, and W. L. Miller (2015), Dissolved organic matter composition and photochemical transformations in the northern North Pacific ocean, *Geophys. Res. Lett.*, *42*, 863–870, doi:10.1002/2014GL062663.

Meybeck, M. (1982), Carbon, nitrogen, and phosphorus transport by world rivers, *Am. J. Sci.*, *282*, 401–450.

Moreira-Turcq, P., P. Seyler, J. L. Guyot, and H. Etcheber (2003), Exportation of organic carbon from the Amazon River and its main tributaries, *Hydrol. Process.*, *17*, 1329–1344.

Moreira-Turcq, P., M.-P. Bonnet, M. Amorim, M. Bernardes, C. Lagane, L. Maurice, M. Perez, and P. Seyler (2013), Seasonal variability in concentration, composition, age, and fluxes of particulate organic carbon exchanged between the floodplain and Amazon River, *Global Biogeochem. Cycles*, *27*, 119–130, doi:10.1002/gbc.20022.

Nohara, D., A. Kitoh, M. Hosaka, and T. Oki (2006), Impact of climate change on river discharge projected by multimodel ensemble, *J. Hydrometeorol.*, *7*, 1076–1089.

Opsahl, S., and R. Benner (1997), Distribution and cycling of terrigenous dissolved organic matter in the ocean, *Nature*, *386*, 480–482.

Opsahl, S., and R. Benner (1998), Photochemical reactivity of dissolved lignin in river and ocean waters, *Limnol. Oceanogr.*, *43*, 1297–1304.

Overland, J. E., and R. W. Preisendorfer (1982), A significance test for principal components applied to a cyclone climatology, *Mon. Weather Rev.*, *110*, 1–4.

Raymond, P. A., and J. E. Bauer (2001), Riverine export of aged terrestrial organic matter to the North Atlantic Ocean, *Nature*, *409*, 497–500.

Raymond, P. A., and R. G. M. Spencer (2015), Riverine DOM, 509–533, in *Biogeochemistry of Marine Dissolved Organic Matter*, 2nd ed., edited by D. Hansell and C. Carlson, pp. 693.

Richey, J. E., R. H. Meade, E. Salati, A. H. Devol, C. F. Nordin Jr., and U. Dos Santos (1986), Water discharge and suspended sediment concentrations in the Amazon River: 1982–1984, *Water Resour. Res.*, *22*, 756–764, doi:10.1029/WR022i005p00756.

Richey, J. E., J. I. Hedges, A. H. Devol, P. D. Quay, R. Victoria, L. Martinelli, and B. R. Forsberg (1990), Biogeochemistry of carbon in the Amazon River, *Limnol. Oceanogr.*, *35*, 352–371.

Šantl-Temkiv, T., K. Finster, T. Dittmar, B. Hansen, R. Thyrhaug, N. Nielsen, and U. Karlson (2013), Hailstones: A window into the microbial and chemical inventory of a storm cloud, *PLoS One*, *8*, e53550, doi:10.1371/journal.pone.0053550.

Seidel, M., M. Beck, T. Riedel, H. Waska, I. G. N. A. Suryaputra, B. Schnetger, J. Niggemann, M. Simon, and T. Dittmar (2014), Biogeochemistry of dissolved organic matter in an anoxic intertidal creek bank, *Geochim. Cosmochim. Acta*, *140*, 418–434.

Sholkovitz, E. R., E. A. Boyle, and N. B. Price (1978), The removal of dissolved humic acids and iron during estuarine mixing, *Earth Planet. Sci. Lett.*, *40*, 130–136.

Smith, W., Jr., and D. J. DeMaster (1996), Phytoplankton biomass and productivity in the Amazon River plume: Correlation with seasonal river discharge, *Cont. Shelf Res.*, *16*, 291–319.

Spencer, R. G. M., et al. (2009), Photochemical degradation of dissolved organic matter and dissolved lignin phenols from the Congo River, *J. Geophys. Res.*, *114*, G03010, doi:10.1029/2009JG000968.

Stubbins, A., R. G. M. Spencer, H. Chen, P. G. Hatcher, K. Mopper, P. J. Hernes, V. L. Mwamba, A. M. Mangangu, J. N. Wabakanghanzi, and J. Six (2010), Illuminated darkness: Molecular signatures of Congo River dissolved organic matter and its photochemical alteration as revealed by ultrahigh precision mass spectrometry, *Limnol. Oceanogr.*, *55*, 1467–1477.

Subramaniam, A., et al. (2008), Amazon River enhances diazotrophy and carbon sequestration in the tropical North Atlantic Ocean, *Proc. Natl. Acad. Sci. U.S.A.*, *105*, 10,460–10,465.

Ward, N. D., R. G. Keil, P. M. Medeiros, D. C. Brito, A. C. Cunha, T. Dittmar, P. L. Yager, A. V. Krusche, and J. E. Richey (2013), Degradation of terrestrially derived macromolecules in the Amazon River, *Nat. Geosci.*, *6*, 530–533.

Welschmeyer, N. (1994), Fluorometric analysis of Chlorophyll *a* in the presence of Chlorophyll *b* and pheopigments, *Limnol. Oceanogr.*, *39*, 1985–1992.

Williams, P. M., and E. R. M. Druffel (1987), Radiocarbon in dissolved organic matter in the central North Pacific Ocean, *Nature*, *330*, 246–248.

Yeung, L. Y., et al. (2012), Impact of diatom-diazotroph associations on carbon export in the Amazon River plume, *Geophys. Res. Lett.*, *39*, L18609, doi:10.1029/2012GL053356.

Ziolkowski, L. A., and E. R. M. Druffel (2010), Aged black carbon identified in marine dissolved organic carbon, *Geophys. Res. Lett.*, *37*, L16601, doi:10.1029/2010GL043963.